Electronic Supplementary Information

Molybdenum Blue Preassembly Strategy to Design Bimetallic $Fe_{0.54}Mo_{0.73}/Mo_2C$@C for Tunable Low-Frequency Electromagnetic Wave Absorption

Peng He,[ade] Runze Ma,[ac] Chen Li,[b] Ling Ran,[ad] Wentao Yuan,[a] Yuyang Han,[de] Lianwen Deng,[b] and Jun Yan*[acde]

[a] College of Chemistry and Chemical Engineering, Central South University, Changsha, 410083, P. R. China
[b] Institute of Super-Microstructure and Ultrafast Process in Advanced Materials, School of Physics and Electronics, Central South University, Changsha, 410083, P. R. China
[c] Hunan Provincial Key Laboratory of Chemical Power Sources, Central South University, Changsha, 410083, P. R. China
[d] Hunan Provincial Key Laboratory of Efficient and Clean Utilization of Manganese Resources, Central South University, Changsha, 410083, P. R. China
[e] Hunan Provincial Key Laboratory of Micro & Nano Materials Interface Science, Central South University, Changsha, 410083, P. R. China

Email: yanjun@csu.edu.cn

Table of Contents

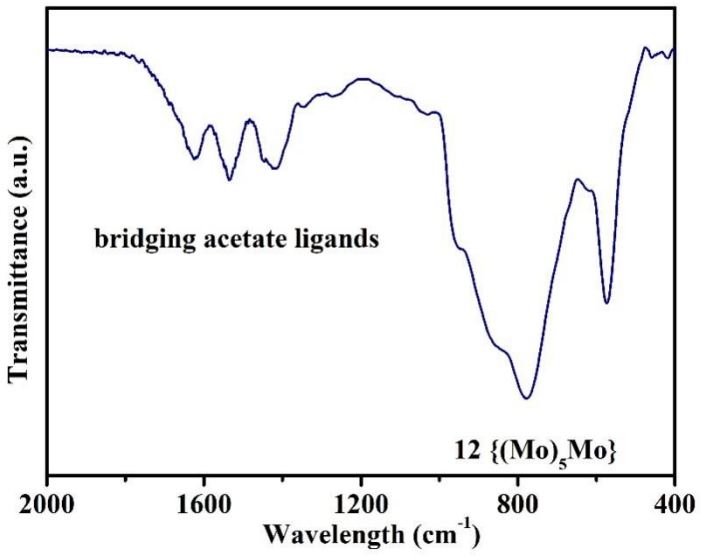

Figure S1. FTIR spectra of $Mo_6 \subset Mo_{72}Fe_{30}$.

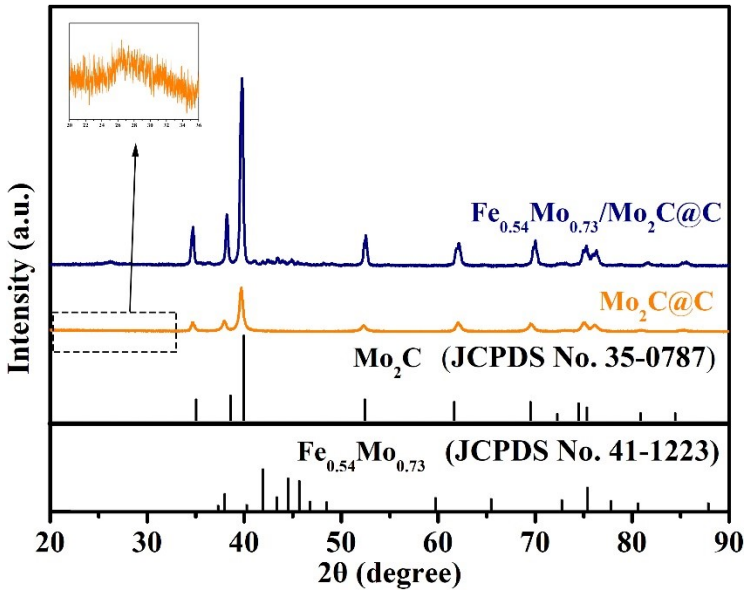

Figure S2. XRD patterns of FMC and MC.

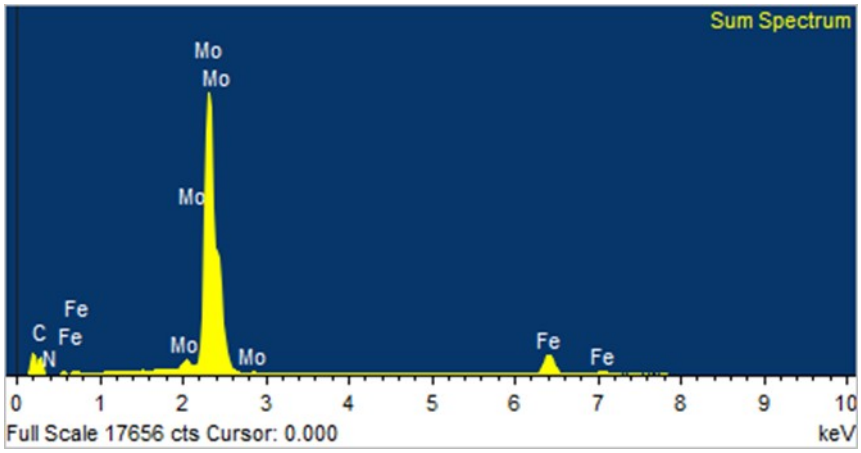

Figure S3. The EDX elemental spectra of FMC.

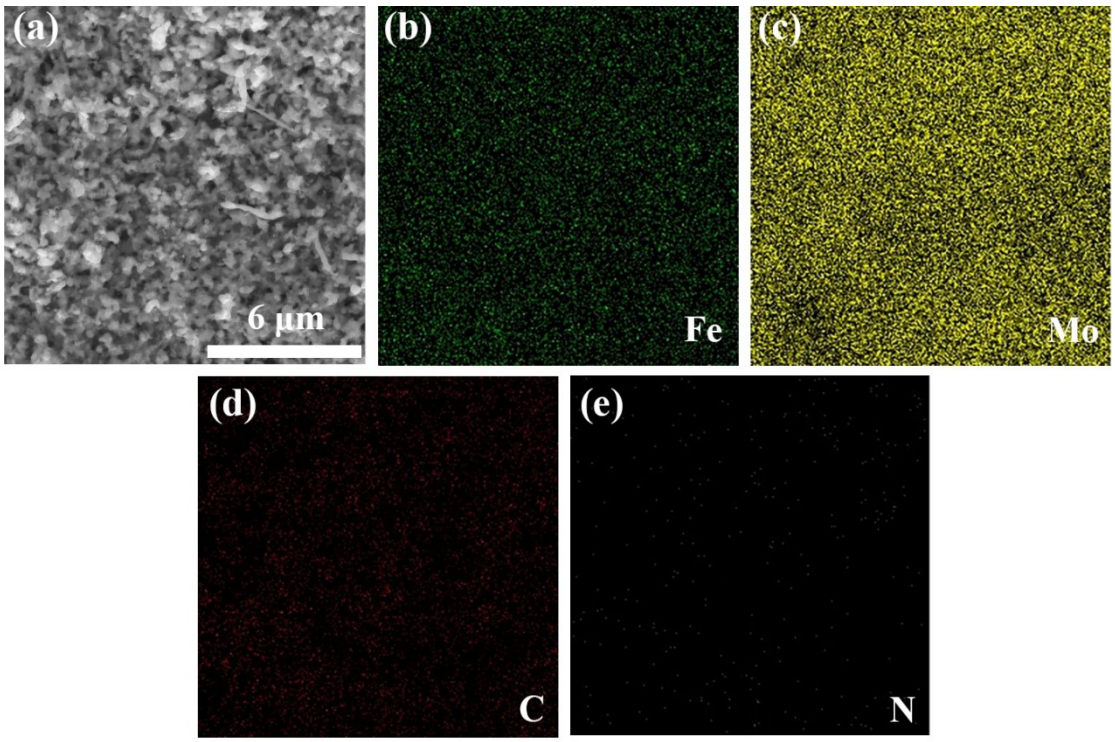

Figure S4. The EDX elemental maps of FMC (a) Corresponding samples, (b) Fe, (c) Mo, (d) C and (e) N.

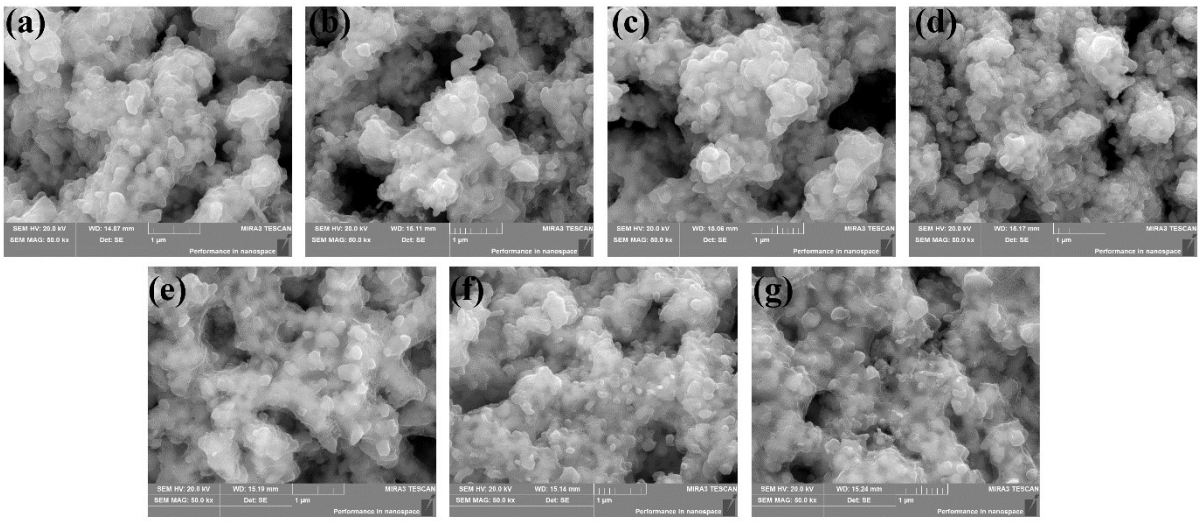

Figure S5. SEM images of (a) FMC-1, (b) FMC-2, (c) FMC-3, (d) FMC-4, (e) FMC-5 and (f) FMC-6.

.

.

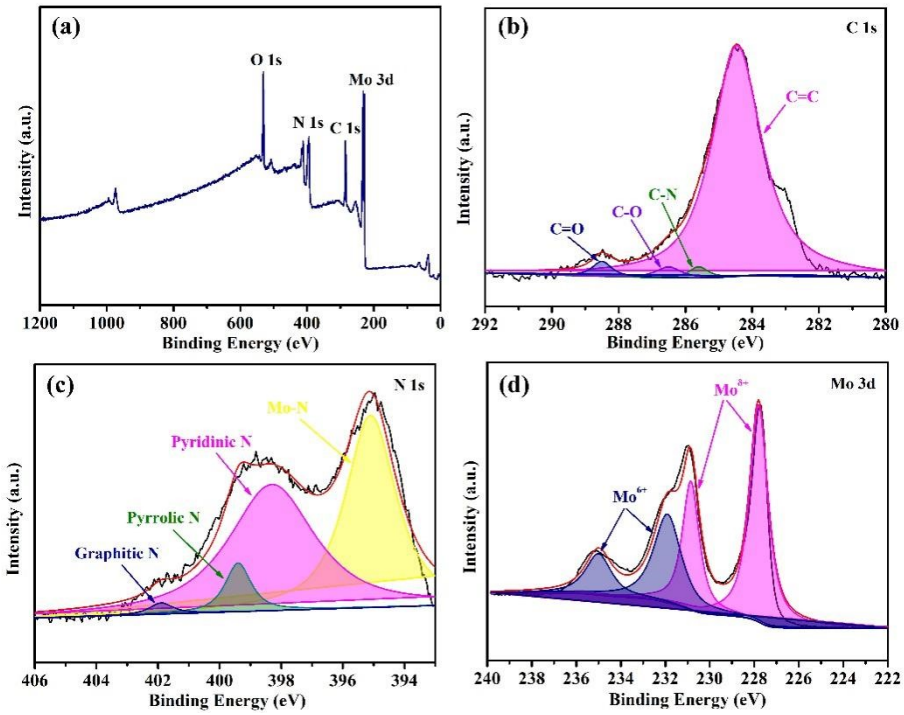

Figure S6. (a) The full XPS spectra of MC. (b-d) High-resolution XPS spectra of MC: (b) C, (c) N and (d) Mo.

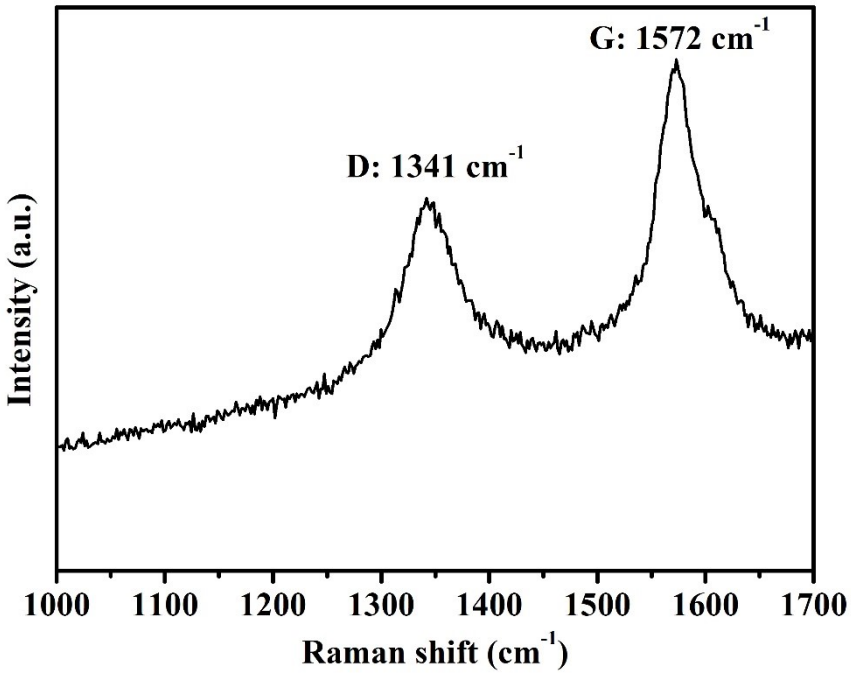

Figure S7. Raman spectra of FMC.

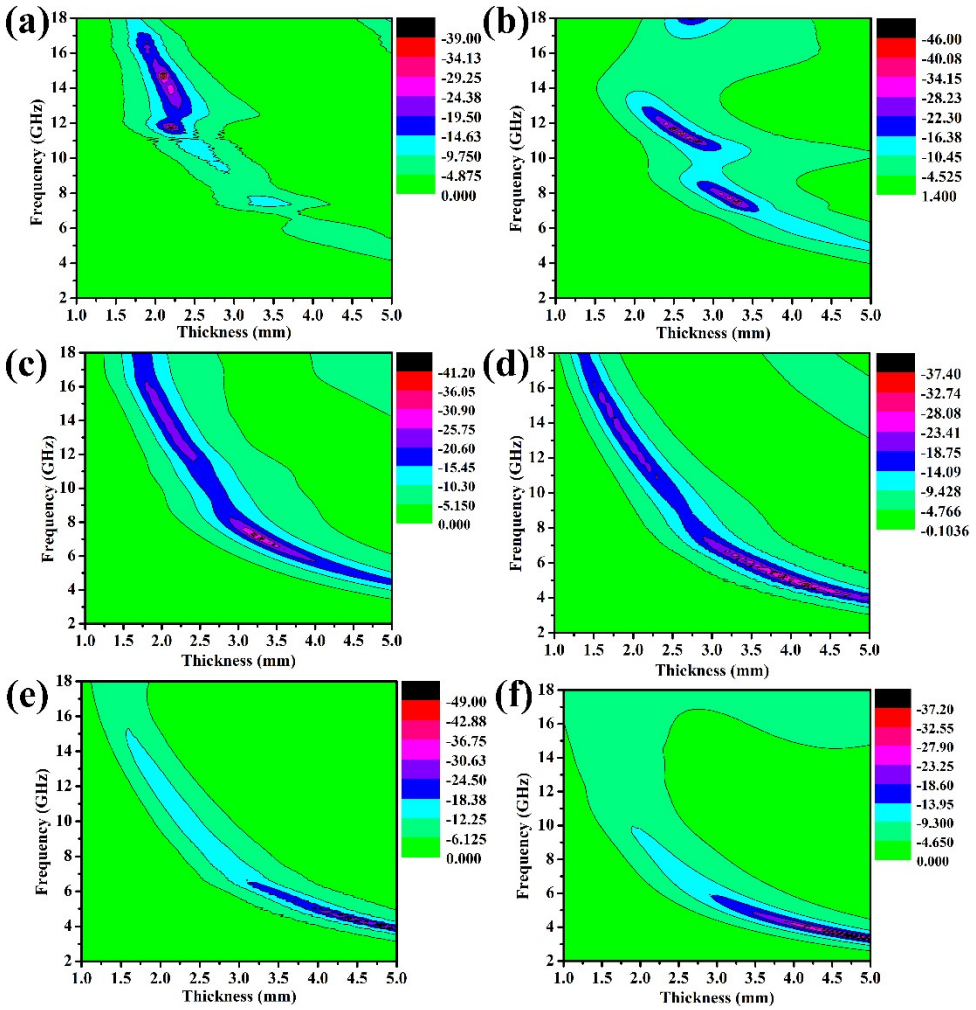

Figure S8. Contour maps depended on the frequency and the thickness of the absorbers for (a) FMC-1, (b) FMC-2, (c) FMC-3, (d) FMC-4, (e) FMC-5 and (f) FMC-6.

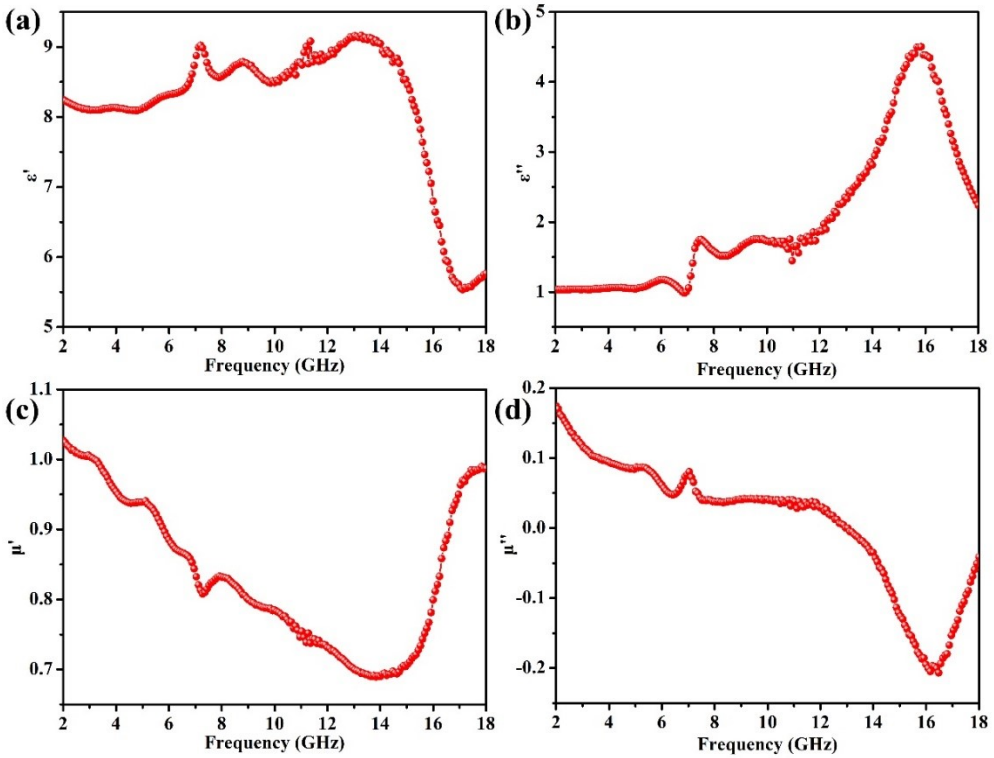

Figure S9. Electromagnetic parameters of MC (the real ε‘ (a) and imaginary ε‘‘ (b) parts of the complex permittivity; the real μ‘ (c) and imaginary μ‘‘ (d) parts of the complex permeability).

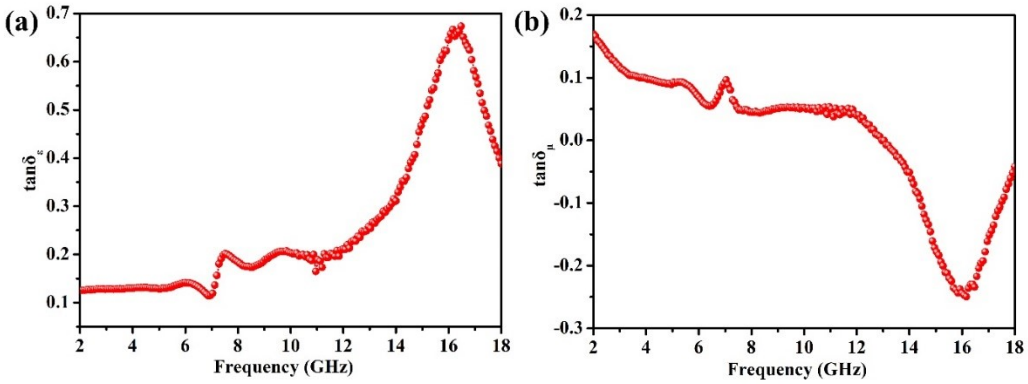

Figure S10. Electromagnetic parameters of MC (dielectric loss $\tan\delta_\varepsilon$ (a), and magnetic loss $\tan\delta_\mu$ (b)).

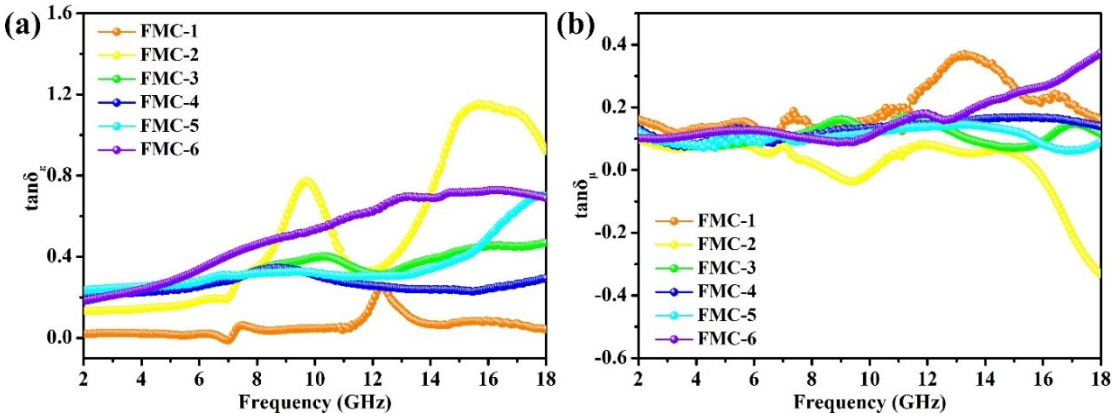

Figure S11. Electromagnetic parameters of FMC composites (dielectric loss $\tan\delta_\varepsilon$ (a), and magnetic loss $\tan\delta_\mu$ (b)).

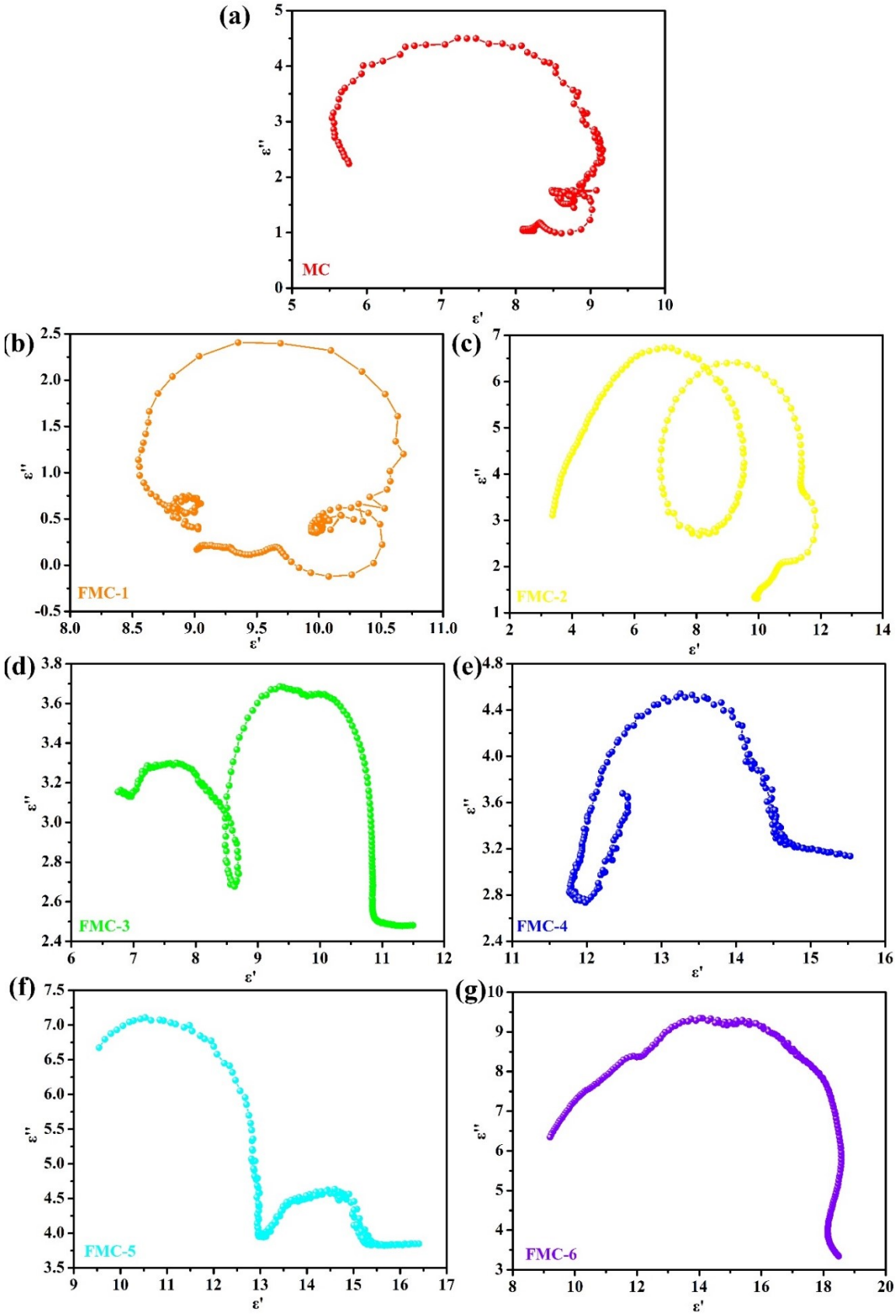

Figure S12. Cole-Cole plots of MC and FMCs.

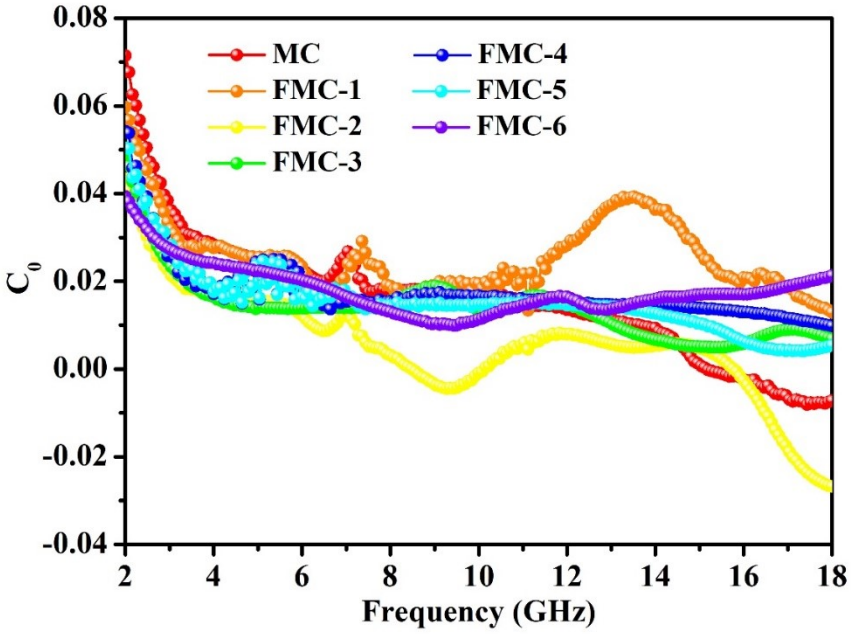

Figure S13. C_0 values of MC and FMCs in the frequency range of 2-18 GHz

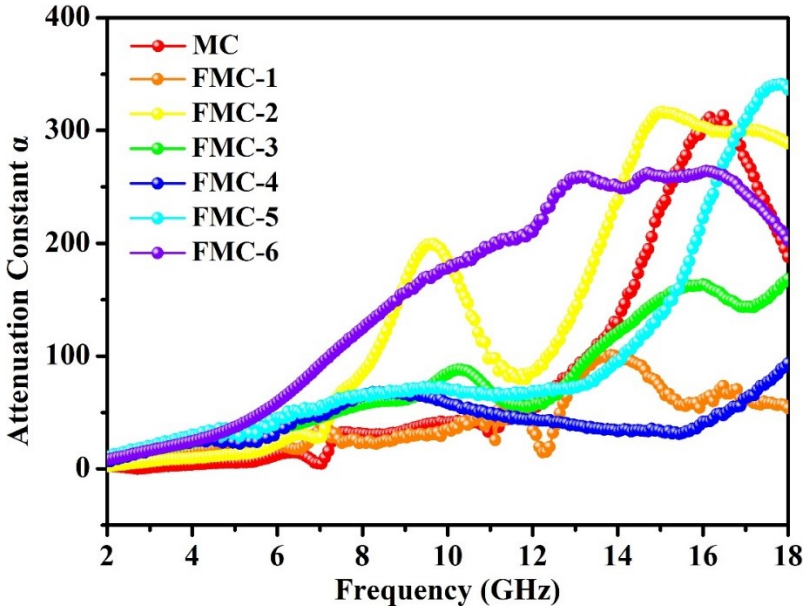

Figure S14. Attenuation constant α of MC and FMCs in the frequency range of 2-18 GHz

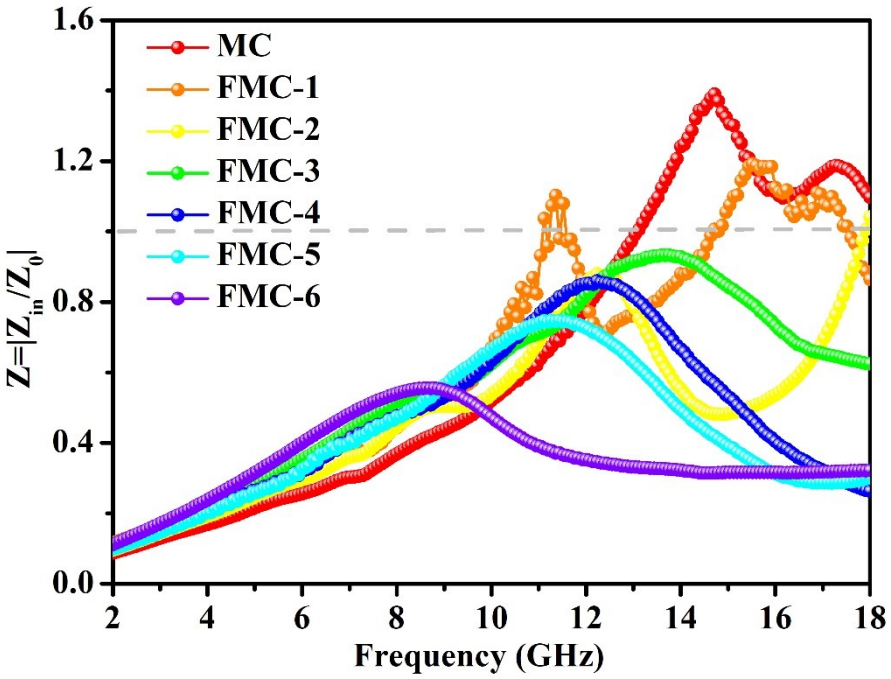

Figure S15. The impedance matching value Z of MC and FMCs in the frequency range of 2-18 GHz

TableS1. ICP–OES results of FMCs

Sample	Fe(mg/L)	Mo(mg/L)	Molar ratio ($Fe_{0.54}Mo_{0.73}/Mo_2C$)
FMC-1	1.935	9.285	2.56
FMC-2	2.144	9.941	2.74
FMC-3	2.413	11.141	2.85
FMC-4	2.670	12.159	2.99
FMC-5	1.893	8.092	3.25
FMC-6	2.389	9.741	3.61

TableS2. Electromagnetic wave absorption of typical carbon-based materials reported in recent literatures.

Band	Materials	Minimum RL (dB)	Frequency (GHz)	Bandwidth range (GHz)	Ref.
Ku band	NiAl-LDH/Graphite	−41.50	17.80	4.40	[1]
	Fe_3N@C	−42.35	17.40	6.00	[2]
	P-doped carbonized bacterial cellulose/$MoSe_2$	−66.84	16.96	10.00	[5]
	Ni/C	−57.25	16.10	5.10	[3]
	C@MoO2/Graphite	−35.40	16.00	4.50	[4]
	FMC-1	−39.00	14.64	5.04	This work
X band	Carbonized bacterial cellulose/MoSe2	−53.33	10.64	4.04	[5]
	CoNSs@RGO	−45.15	10.52	7.14	[6]
	Graphene/ Si_3N_4	−23.50	9.27	4.20	[7]
	Mo_2C/C	−49.19	9.04	4.56	[8]
	$Mo_{4.8}Si_3C_{0.6}/SiC/C_{free}$	−59.00	8.00	12.55	[9]
	FMC-2	−45.92	11.68	3.28	This work
C band	$Co_9S_8/C/Ti_3C_2T_x$	−50.07	7.60	4.24	[10]
	C@MoO2/Graphite	−33.50	6.90	4.88	[4]
	Mo_2C/Co/C	−48.00	6.60	15.00	[11]
	CoNC/CNTs	−44.60	5.20	4.50	[12]
	FMC-5	−48.91	4.08	1.04	This work
S band	Ni/MWCNT	−24.90	2.80	—	[13]
	FMC-6	−37.15	3.52	0.8	This work

References

1 X. F, Xu, S. H. Shi, Y. L. Tang, G. Z. Wang, M. F. Zhou, G. Q. Zhao, X. C. Zhou, S. W. Lin, F. B. Meng, Growth of NiAl-Layered Double Hydroxide on Graphene toward Excellent Anticorrosive Microwave Absorption Application. *Adv. Sci.,* 2021, **8**, 2002658.

2 X. Q. Cui, X, H. Liang, W. Liu, W. H. Gu. G. B. Ji and Y. W. Du, Stable microwave absorber derived from 1D customized heterogeneous structures of Fe_3N@C. *Chem. Eng. J.,* 2020, **381**, 122589.

3 Y. Qiu, Y. Lin, H. B. Yang, L. Wang, M. Q. Wang and B. Wen, Hollow Ni/C microspheres derived from Ni-metal organic framework for electromagnetic wave absorption. *Chem. Eng. J.,* 2020, **383**, 123207.

4 C. Wu, Z. F Chen, M. L. Wang, X. Cao, Y. Zhang, P. Song, T. Y. Zhang, X. L. Ye, Y. Yang, W. H. Gu, J. D. Zhou, Y. Z. Huang, Confining Tiny MoO_2 Clusters into Reduced Graphene Oxide for Highly Efficient Low Frequency Microwave Absorption. *Small,* 2020, **16**, 2001686.

5 Z. J. Xu, M. He, Y. M. Zhou, S. X. Nie, Y. J. Wang, Y. Huo, Y. F. Kang, R. L. Wang, R. Xu, H. Peng, X. Chen, Spider web-like carbonized bacterial cellulose/$MoSe_2$ nanocomposite with enhanced microwave attenuation performance and tunable absorption bands. *Nano Res.,* 2021, **14**, 738-746.

6 Y. Ding, Z. Zhang, B. Luo, Q. Liao, S. Liu, Y. Liu, Y. Zhang, Investigation on the broadband electromagnetic wave absorption properties and mechanism of Co_3O_4-nanosheets/reduced-graphene-oxide composite. *Nano Res.,* 2017, **10**, 980-990.

7 F. Ye, Q. Song, Z. C. Zhang, W. Li, S. Y. Zhang, X. W. Yin, Y. Z. Zhou, H. W. Tao, Y. S. Liu, L. F. Cheng, L. T. Zhang, H. J. Li, Direct Growth of Edge-Rich Graphene with Tunable Dielectric Properties in Porous Si_3N_4 Ceramic for Broadband High-Performance Microwave Absorption. *Adv. Funct. Mater.,* 2018, **28**, 1707205.

8 S. S. Dai, Y. Cheng, B. Quan, X. H. Liang, W. Liu, Z. H. Yang, G. B. Ji and Y. W. Du, Porous-carbon-based Mo2C nanocomposites as excellent microwave absorber: a new exploration. *Nanoscale,* 2018, **10**, 6945-6953.

9 Y. Feng, Y. j. Yang, Q. B. Wen, R. Riedel, Z. J. Yu, Dielectric Properties and Electromagnetic Wave Absorbing Performance of Single-Source-Precursor Synthesized $Mo_{4.8}Si_3C_{0.6}/SiC/C_{free}$ Nanocomposites with an In Situ Formed Nowotny Phase. *ACS Appl. Mater. Interfaces,* 2020, **12**, 16912-16921.

10 T. Q. Hou, Z. R. Jia, B. B. Wang, H. B. Li, X. H. Liu, L. Bi, G. L. Wu, MXene-based accordion 2D hybrid structure with $Co_9S_8/C/Ti_3C_2T_x$ as efficient electromagnetic wave absorber. *Chem. Eng. J.,* 2021, **414**, 128875.

11 Y. H. Wang, X. D. Li, X. J. Han, P. Xu, L. R. Cui, H. H Zhao, D. W. Liu, F. Y. Wang and Y. C. Du, Ternary Mo_2C/Co/C composites with enhanced electromagnetic waves absorption. *Chem. Eng. J.,* **2020**, *387*, 124159.

12 X. Q. Xu, F. T. Ran, Z. M. Fan, H. Lai, Z. J. Cheng, T. Lv, L. Shao, Y. Y. Liu, Cactus-Inspired Bimetallic Metal–Organic Framework-Derived 1D–2D Hierarchical Co/N-Decorated Carbon Architecture toward Enhanced Electromagnetic Wave Absorbing Performance. *ACS Appl. Mater. Interfaces,* 2019, **11**, 13564-13573.

13 G. Tong, F. Liu, W. Wu, F. Du and J. G. Guan, Rambutan-like Ni/MWCNT heterostructures: Easy synthesis, formation mechanism, and controlled static magnetic and microwave electromagnetic characteristics. *J. Mater. Chem. A,* 2014, **2**, 7373-7382.